Biochimica et Biophysica Acta, 689 (1982) 531–538
Elsevier Biomedical Press

BBA 71270

INTERACTION OF PHLORETIN WITH THE ANION TRANSPORT PROTEIN OF THE RED BLOOD CELL MEMBRANE

STUART A. FORMAN, A.S. VERKMAN, JAMES A. DIX * and A.K. SOLOMON

Biophysical Laboratory, Department of Physiology and Biophysics, Harvard Medical School, Boston, MA 02115 (U.S.A.)

(Received September 1st, 1981)
(Revised manuscript received April 1st, 1982)

Key words: Anion transport inhibition; Phloretin; Band 3 protein; Kinetics; (Erythrocyte membrane)

Phloretin is an inhibitor of anion exchange and glucose and urea transport in human red cells. Equilibrium binding and kinetic studies indicate that phloretin binds to band 3, a major integral protein of the red cell membrane. Equilibrium phloretin binding has been found to be competitive with the binding of the anion transport inhibitor, 4,4′-dibenzamido-2,2′-disulfonic stilbene (DBDS), which binds specifically to band 3. The apparent binding (dissociation) constant of phloretin to red cell ghost band 3 in 28.5 mM citrate buffer, pH 7.4, 25°C, determined from equilibrium binding competition, is 1.8±0.1 μM. Stopped-flow kinetic studies show that phloretin decreases the rate of DBDS binding to band 3 in a purely competitive manner, with an apparent phloretin inhibition constant of 1.6±0.4 μM. The pH dependence of equilibrium binding studies show that it is the charged, anionic form of phloretin that competes with DBDS binding, with an apparent phloretin inhibition constant of 1.4 μM. The phloretin binding and inhibition constants determined by equilibrium binding, kinetic and pH studies are all similar to the inhibition constant of phloretin for anion exchange. These studies suggest that phloretin inhibits anion exchange in red cells by a specific interaction between phloretin and band 3.

Introduction

Phloretin(3-(4-hydroxyphenyl)-1-(2,4,6-trihydroxyphenyl)-1-propanone) exhibits diverse effects on transport processes across the human red cell membrane. Phloretin appears to accelerate transport through membrane lipids [1,2] including lipophilic nonelectrolyte permeability, valinomycin-mediated potassium flux, and transport of acetate in the undissociated form. On the other hand, phloretin inhibits protein mediated processes in the red cell, including glucose and anion transport; phloretin is also a potent inhibitor of the transport of small, hydrophilic, nonelectrolytes [2–5]. The bimodal effect of phloretin may be related to the two distinct classes of phloretin binding sites on the red cell membrane [6], a protein class ($K_d = 1.5$ μM, $2.5 \cdot 10^6$ sites/cell) and a lipid class ($K_d = 54$ μM, $5.5 \cdot 10^7$ sites/cell).

In order to study the protein class of sites, specific interactions of phloretin with band 3, the anion-exchange protein of the red cell, have been studied using a stilbene inhibitor of anion exchange. DIDS (4,4′-diisothiocyano-2,2′-disulfonic stilbene) is the anion-exchange inhibitor that has been most widely characterized [7]; we have used DBDS (4,4′-dibenzamido-2,2′-disulfonic stilbene),

* Present address: Department of Chemistry, SUNY Binghamton, Binghamton, NY 13901, U.S.A.

Abbreviations: DBDS, 4,4′-dibenzamido-2,2′-disulfonic stilbene; DIDS, 4,4′-diisothiocyano-2,2′-disulfonic stilbene.

0005-2736/82/0000–0000/$02.75

an analogue of DIDS, which fluoresces [8] when bound to band 3. More than 99% of the DBDS binding is inhibited when DIDS is covalently bound to band 3 in red cell ghost membranes. DBDS fluorescence has been shown to be an indicator of the band 3 conformational state [9]. Evidence is presented which shows a simple competition between phloretin and DBDS for a binding site on band 3 and suggests that this competition may be responsible for the observed inhibition of anion exchange by phloretin.

Materials and Methods

Phloretin was purchased from K and K Laboratories (Plainview, NY) and its purity was checked by thin-layer chromatography in chloroform/propanol (3:1, v/v). Phloretin was dissolved in 1 M NaOH and added to buffer which was subsequently titrated to pH 7.4. DBDS was synthesized by the method of Kotaki et al. [10].

Human red cell ghosts were prepared by the method of Dodge et al. [11] from recently outdated bank blood. All experiments were performed in 28.5 mM sodium citrate buffer at pH 7.4 (160 mM ionic strength) to minimize interactions with transportable anions. Schnell et al. [12] have concluded that citrate exercises little effect on the concentration dependence of chloride self-exchange (see also Ref. 7) and we have found [9] that the replacement of citrate with gluconate has little effect on DBDS binding. pH dependence studies were done in sodium citrate-glycylglycine buffer. Protein concentrations were measured by the method of Lowry et al. [13].

Stopped-flow experiments were performed on an apparatus consisting of two hand-driven syringes which propel solutions into a dual-jet stream mixing chamber and quartz observation cell as previously described [14,15]. Equilibrium fluorescence intensities were measured on a Perkin-Elmer MFP-2A spectrofluorometer (Norwalk, CT) interfaced to a DEC PDP 11/34 (Maynard, MA) computer [16] at an excitation of 356 nm and emission of 426 nm. Equilibrium binding measurements were performed by measuring the fluorescence of a dilute ghost membrane solution (0.04 mg/ml ghost protein) when known concentrations of DBDS were added. The fluorescence intensity was taken to represent the amount of DBDS bound to the membrane [9], after correction for ghost scattering, unbound solution DBDS and inner filter effects (correction for self absorption of excitation and emission light by DBDS). In equilibrium binding experiments, phloretin was added to the ghost solution prior to the addition of DBDS. In stopped-flow experiments, phloretin was added to both DBDS and ghost solutions.

Results and Discussion

Equilibrium binding studies

In the absence of phloretin, the mechanism of binding of DBDS to band 3 (b3) in ghost membranes is [9]:

$$\mathrm{b3} \underset{\mathrm{DBDS}}{\overset{K_1}{\rightleftharpoons}} \mathrm{b3\text{-}DBDS} \overset{K_2}{\leftrightarrow} \mathrm{b3^{*}\text{-}DBDS} \underset{\mathrm{DBDS}}{\overset{K_3}{\rightleftharpoons}} \mathrm{b3^{*}\text{-}(DBDS)_2} \qquad (1)$$

in which b3-DBDS and b3*-DBDS represent different conformational states of the complex. The measured equilibrium constants (K_1^{eq} and K_2^{eq}) for the binding of the first and second DBDS molecules to band 3 in the sequential mechanism above (Eqn. 1) each contain contributions from two individual steps, as given below. The two equilibrium (dissociation) binding constants * are related to K_1, K_2 and K_3, by

$$K_1^{eq} = K_1/(1 + K_2) \qquad (2)$$

$$K_2^{eq} = K_3(1 + (1/K_2)) \qquad (3)$$

Typical fluorescence probe binding data in the presence of phloretin are shown in Fig. 1. In the

* The notation for the equilibrium binding (dissociation) constants used in this paper is:

K_1, K_2, K_3, equilibrium constants for the individual steps of the DBDS binding mechanism in Eqn. 1.

K_1^{eq}, K_2^{eq}, experimentally determined equilibrium constants for DBDS binding in the absence of phloretin.

$(K_1)_{app}$, apparent dissociation constant for the first bimolecular step in the presence of phloretin.

$(K_1^{eq})_{app}$, apparent equilibrium constant for DBDS binding in the presence of phloretin.

K_i^{app}, apparent inhibition constant of phloretin in the presence of DBDS.

presence of 50 μM phloretin, the affinity of the first, high-affinity DBDS-binding site decreases dramatically, as shown by the decreased initial slope of the fluorescence binding curve in the top portion of Fig. 1. The affinity of the second, low-affinity binding site also decreases, although the data that define this site are not precise due to large inner filter corrections at high [DBDS]. In the bottom half of Fig. 1, the fluorescence binding data have been replotted in the form of a Scatchard plot to exhibit the effect of phloretin more clearly. The Scatchard plots were made assuming the total stoichiometry of DBDS binding was not changed in the presence of phloretin. This assumption is supported by the observation that the fluorescence intensity of DBDS bound to ghost membranes, extrapolated to infinite probe concentration and corrected for inner filter effects, was independent of phloretin concentration. The Scatchard plot shows quite dramatically that phloretin decreases the affinity for DBDS binding.

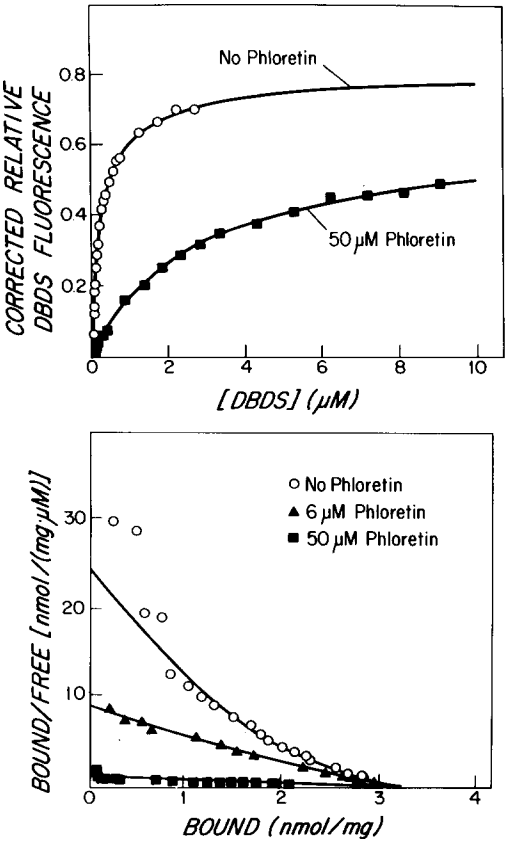

Fig. 1. Effect of phloretin on DBDS binding to ghost membranes. Top: The fluorescence of solutions containing known concentrations of phloretin and 0.04 mg/ml ghost protein in 28.5 mM sodium citrate, pH 7.4, 25°C was measured as a function of DBDS concentration. Bottom: Fluorescence binding data are plotted in the form of a Scatchard plot with a DBDS binding stoichiometry [9] of 3.2 μM/(mg/ml). Fitted curves for top and bottom were obtained by non-linear least-squares regression to a two-site sequential binding mechanism.

Binding data were analyzed by non-linear least-squares using a two site sequential model,

$$\frac{\nu}{[\mathrm{DBDS}]} = \frac{n(K_2^{eq} + [\mathrm{DBDS}])}{K_1^{eq}K_2^{eq} + 2K_2^{eq}[\mathrm{DBDS}] + [\mathrm{DBDS}]^2} \quad (4)$$

where ν is the amount of probe bound, n is the total stoichiometry and K_1^{eq} and K_2^{eq} are the experimentally determined equilibrium constants for sites 1 and 2 in the absence of phloretin. Fig. 2 shows the dependence of $(K_1^{eq})_{app}$, the value of K_1^{eq} in the presence of phloretin, on phloretin

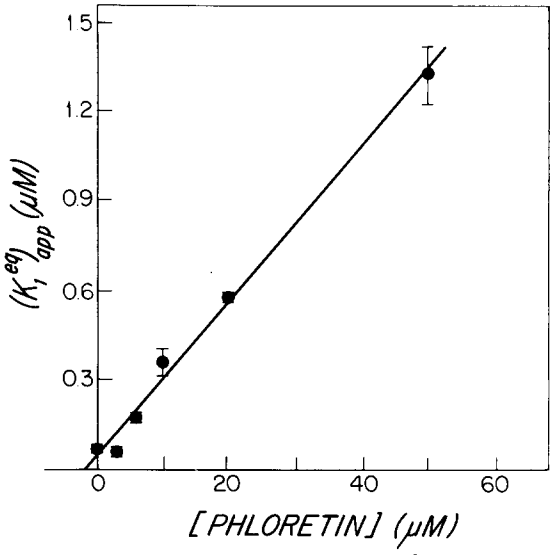

Fig. 2. Effect of phloretin on apparent equilibrium binding constants of DBDS to ghost membranes. The high affinity equilibrium binding constant is plotted against total phloretin concentration at pH 7.4, 25°C in 28.5 mM sodium citrate. Error bars represent one standard deviation from the mean; the fitted line was obtained by a weighted least-squares fit to the data. The negative x-intercept, 1.8±0.3 μM, gives K_i for phloretin inhibition of DBDS binding.

concentration at pH 7.4, 25°C. If binding of phloretin is competitive with probe binding, a plot of $(K_1^{eq})_{app}$ vs. phloretin concentration ([Phl]) should be a straight line with an x-intercept of $-K_i$,

$$(K_1^{eq})_{app} = K_1^{eq}\left(1 + \frac{[Phl]}{K_i}\right) \quad (5)$$

The data in Fig. 2 are consistent with simple competitive inhibition with a phloretin K_i of 1.8 ± 0.3 μM. The inhibition constant K_i agrees with the value of K_d (1.5 μM) for the high-affinity phloretin site on red cell membranes [6].

Stopped-flow studies

Since K_1^{eq} is determined by two parameters (see Eqn. 2), the effect of phloretin (Fig. 2) may be due either to an effect on K_1 or K_2. An effect on K_1 would suggest simple competition for a single site. An effect on K_2, a step in which no competitive interaction is possible, would suggest an allosteric effect on the protein, as has been seen with chloride [17]. Equilibrium measurements can not differentiate between these alternatives, whereas stopped-flow kinetic experiments can determine the values of K_1 and K_2 separately.

Fig. 3 shows the effect of 20 μM phloretin on the time course of DBDS binding to ghosts as measured in a stopped-flow experiment. Phloretin both decreases the amplitude and the rate of DBDS binding to ghosts in the stopped-flow trace, consistent with simple competition for a single binding site. Time constants were obtained from non-linear least-squares fits of single exponential functions to the stopped-flow traces. These are plotted in Fig. 4 against reciprocal DBDS concentration for several phloretin concentrations. This plot is similar to a Michaelis-Menten plot in which the inverse velocity is given by the stopped-flow time constant. The data at high DBDS concentrations appear to intersect at a single point on the y axis. Thus, phloretin appears to interact with DBDS by a simple competitive mechanism, in contrast to a non-competitive mechanism in which the y-intercept would vary with phloretin concentration. A detailed, non-linear fit of the stopped-flow data, as described previously [9,18], allows resolution of the equilibrium constants, K_1 and K_2, for DBDS binding to ghosts.

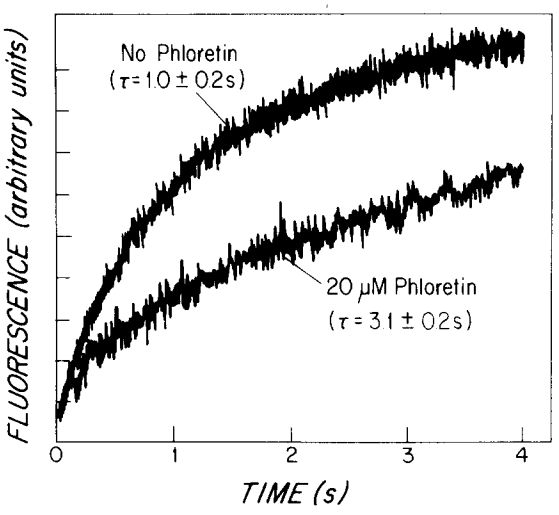

Fig. 3. Effect of phloretin on time-course of DBDS binding to ghosts. In a stopped-flow experiment, 1 μM DBDS was mixed with ghosts (0.04 mg/ml ghost protein) in 28.5 mM sodium citrate, pH 7.4, 25°C. In the bottom trace, 20 μM phloretin was present in each solution prior to mixing.

If the interaction between phloretin and DBDS were simple competition for a single binding site, then phloretin should increase the apparent value

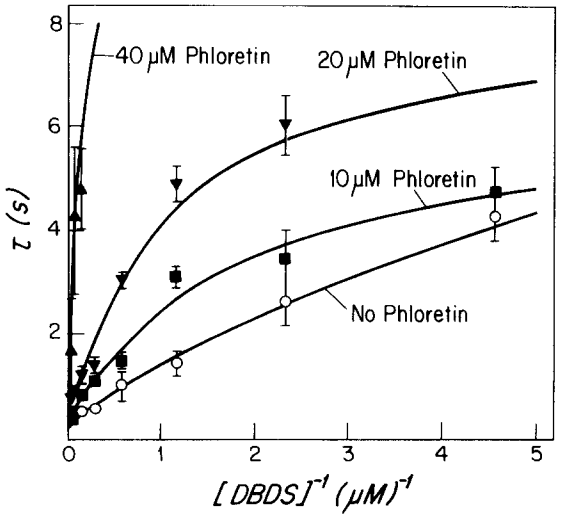

Fig. 4. Effect of phloretin on the kinetics of DBDS binding to ghosts. Each point represents the average from experiments performed in quadruplicate; error bars are one standard deviation from the mean. Fitted curves were obtained from a fit to kinetic equations describing sequential binding of DBDS to band 3 according to Eqn. 1 [9,18].

of K_1 without affecting K_2,

$$\text{b3-Phl} \overset{K_i}{\underset{\text{Phl}}{\rightleftharpoons}} \text{b3} \overset{K_1}{\underset{\text{DBDS}}{\rightleftharpoons}} \text{b3-DBDS} \overset{K_2}{\leftrightarrow} \text{b3}^*\text{-DBDS}$$

$$\overset{K_3}{\underset{\text{DBDS}}{\rightleftharpoons}} \text{b3}^*\text{-(DBDS)}_2 \qquad (6)$$

The apparent dissociation constant of the first bimolecular step, $(K_1)_{app}$, is

$$(K_1)_{app} = K_1\left(1 + \frac{[\text{Phl}]}{K_i}\right) \qquad (7)$$

The slope of the top curve in Fig. 5, given in the legend, does not differ significantly from 0, showing that phloretin does not affect the value of K_2, 36 ± 10. $(K_1)_{app}$ is linearly dependent on phloretin concentration and equals $(1.6[\text{Phl}] + 3)$ μM. The value of K_i calculated from Eqn. 7 is 1.6 ± 0.4 μM, consistent with $K_i = 1.8 \pm 0.3$ μM calculated above from the effect of phloretin on equilibrium DBDS binding.

Since the fitted curves in Fig. 4 have approximately the same intercept on the τ axis, phloretin binds competitively with DBDS for a single site on band 3. If phloretin could bind simultaneously with DBDS to another site on band 3, one would expect that, as [DBDS] $\rightarrow \infty$, the time constant of the band 3-DBDS conformational change would be dependent on phloretin concentration. As Fig. 4 shows, this is not the case. Furthermore, if there were an independent site for phloretin on band 3, the reaction scheme in Eqn. 6 would not be correct. The value for K_i obtained from kinetic measurements depends upon the validity of Eqns. 6 and 7 so that the agreement between the phloretin-inhibition constants for DBDS binding as obtained in equilibrium and stopped-flow measurements constitutes strong evidence that phloretin binds competitively with DBDS for a single site.

Phloretin is a weak acid, with a pK_a of 7.3. In order to determine whether the charged or uncharged form of phloretin is active in the inhibition of DBDS equilibrium binding to ghosts, the pH dependence of phloretin competition with DBDS was measured as shown in Fig. 6. As pH increases, the difference between the effect of the

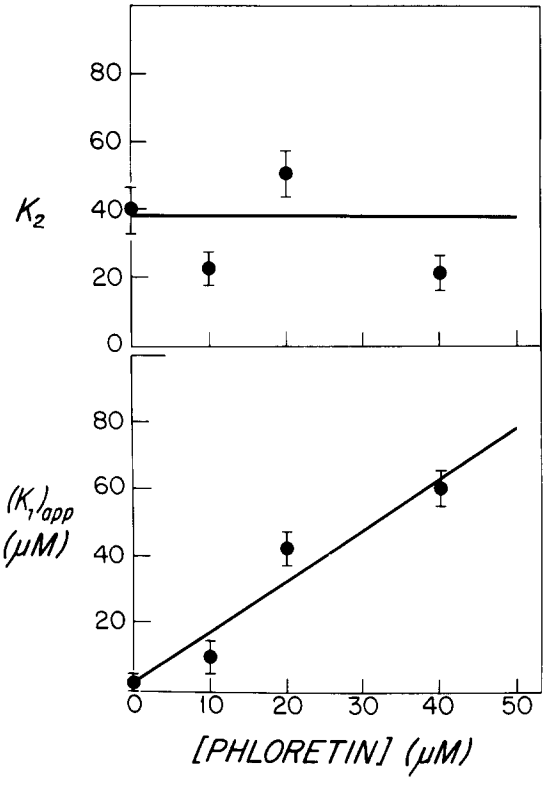

Fig. 5. Effect of phloretin on equilibrium constants of DBDS binding to ghosts. The slope for the top line is -0.2 ± 0.5 μM^{-1} and the intercept is 36 ± 10. The slope for the bottom line is 1.6 ± 0.2 and the intercept is 3 ± 2 μM. Error bars represent one standard deviation.

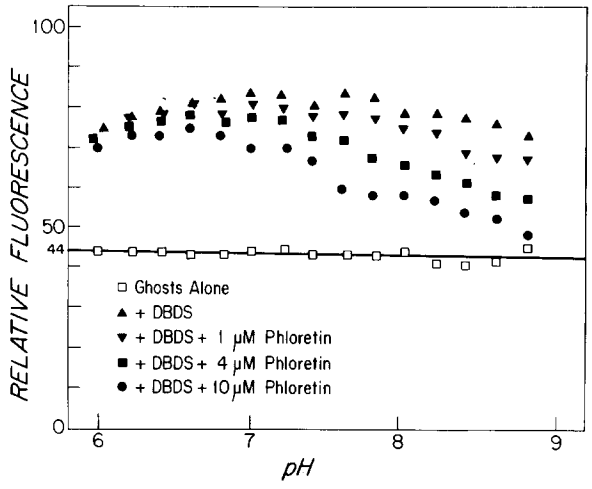

Fig. 6. pH dependence of phloretin effect on DBDS binding to ghosts. The fluorescence of a solution, containing 200 nM DBDS, ghosts (0.04 mg/ml ghost protein) and varying phloretin concentrations, was measured as a function of pH. The buffer consisted of 25 mM glycylglycine + 24 mM sodium citrate, 25°C.

lowest and highest total phloretin concentration on DBDS binding becomes more pronounced. Since the charged form predominates at higher pH values, these observations suggest that the charged form of phloretin is active. This can be illustrated more clearly by comparing the dependence of the relative fluorescence data on either the concentration of uncharged phloretin ([HPhl], Fig. 7, top), or charged phloretin ([Phl^-], Fig. 7, bottom). For the uncharged form, the data fall along curves which suggest that increased uncharged phloretin causes increased DBDS binding. Since these curves are separate, [HPhl] cannot be the proper independent variable to describe phloretin inhibition of DBDS binding. When plotted against the concentration of charged phloretin, it becomes clear that the fraction bound decreases monotonically as a function of charged phloretin. The data appear to follow a single line with an apparent half-inhibition constant, K_i^{app}, of 5.5 ± 2.4 μM, indicating that charged phloretin is the correct independent variable. K_i^{app} is related to K_i for phloretin by

$$K_i^{app} = K_i\left(1 + \frac{[DBDS]}{K_I^{eq}}\right) \tag{8}$$

Since 200 nM DBDS was used in these experiments, the K_i^{app} of 5.5 ± 2.4 μM corresponds to a K_i of 1.4 ± 0.6 μM, given the measured value of 65 nM for K_I^{eq} for DBDS binding in the absence of phloretin [9].

The conclusion that the charged form of phloretin is active in the inhibition of DBDS binding is valid provided that the binding of probe to ghosts in the absence of phloretin is not strongly pH dependent. A control binding experiment performed at pH 8.4 gave $K_I^{eq} = 110 \pm 40$ nM [9], in the same general range as the value $K_I^{eq} = 65 \pm 8$ nM obtained at pH 7.4 [9]. The value of K_i determined by the pH dependence of phloretin binding is in good agreement with the values already presented for determination by equilibrium binding and kinetic analysis as shown in Table I. As the table shows, the present values also agree with those previously given by Wieth et al. [19] for inhibition of anion transport and Jennings and Solomon [6] for binding to the phloretin high affinity site. Simple competition between phloretin

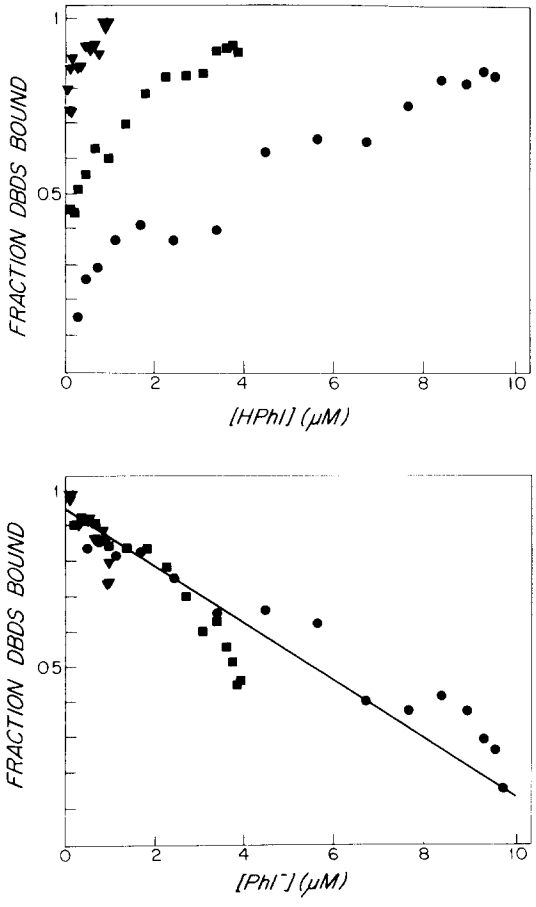

Fig. 7. Charge dependence of phloretin inhibition of DBDS binding. The data from Fig. 6 were plotted as a function of the concentration of charged and uncharged forms of phloretin to determine the active form of phloretin. Top: The fraction of DBDS bound is plotted against the concentration of uncharged phloretin (same symbols as in Fig. 6). Bottom: The fraction of DBDS bound is plotted against the concentration of charged phloretin.

TABLE I

K_i FOR PHLORETIN INTERACTION ON RED CELL MEMBRANE PROTEIN

Method	K_i (μM)	Reference
Equilibrium binding	1.5 ± 1.0	Jennings and Solomon [6]
Anion-exchange inhibition	2–5	Wieth et al. [19]
DBDS equilibrium binding	1.8 ± 0.3	Present study
DBDS kinetic analysis	1.6 ± 0.4	Present study
DBDS equilibrium binding, pH dependence	1.4 ± 0.6	Present study

and probe by equilibrium and kinetic measurements places the probable binding site for phloretin at or near the probe-binding site. Jennings and Solomon [6] found $(2.5 \pm 1.5) \cdot 10^6$ high-affinity protein-binding sites for phloretin on the red cell membrane. The present studies show that phloretin, a potent inhibitor of anion transport, has specific binding sites on band 3, the anion exchange protein. Since there are $1.2 \cdot 10^6$ copies of band 3 present on the red cell membrane, there may remain additional, non-band 3, high-affinity protein-binding sites for phloretin. If so, these additional sites must have the same affinity as the others since Jennings and Solomon [6] have shown only a single class of high-affinity site.

Since binding of DBDS appears to be non-competitive with chloride binding [17], simple competition between phloretin and DBDS would predict non-competitive inhibition of anion transport by phloretin. Recent experiments (Fröhlich, O., personal communication) show that phloretin inhibits chloride self-exchange in human red cells in a mixed competitive manner, consistent with the present study.

Cousin and Motais [20] have suggested that phloretin exerts its inhibitory effects on anion, nonelectrolyte and glucose transport through an interaction with the membrane lipid. Since phloretin alters the internal membrane electric potential when bound to lipid binding sites near the lipid headgroups [21,22], it would be possible for it to alter the function of a transmembrane protein by altering electric potential. However, the present finding of simple competition between phloretin and DBDS on band 3 is not consistent with this picture. Furthermore, it is unlikely that the DBDS competition can be due to phloretin binding to the lipid annulus since phloretin binding to red cell lipid has a K_d of 54 μM [6], very different from the 1.4–1.8 μM value of K_d found in the present study. Moreover, it is the charged form of phloretin which is active in DBDS binding inhibition, so that it would be necessary for Phl^- to bind to annulus lipids. However, Verkman and Solomon [23] showed that Phl^- binding to lipid is less tight than HPhl binding by a factor of 10^3, making it unlikely that there is significant binding of phloretin to lipids at the low concentrations used in this study.

It is not surprising that the negatively charged form of phloretin competes simply with DBDS on band 3. Both molecules are negatively charged, and share regions of striking structural similarity as shown in Fig. 8. The mechanism of phloretin inhibition of stilbene binding could be steric hindrance if the stilbene binding site is located in a deep cleft in band 3 in the vicinity of the chloride binding site as proposed by Macara and Cantley [24].

It is important to realize, however, that the present study, by itself, cannot rule out binding and functional effects of the uncharged form of phloretin at high affinity sites on band 3 or in the lipid annulus, since DBDS-band 3 conformational states may not be sensitive there. It is unlikely that a significant lipid effect on anion transport exists since Jennings and Solomon found that the K_d for phloretin binding to lipids was 54 μM, more than an order of magnitude greater than the concentration of phloretin needed to inhibit anion exchange and affect DBDS binding and kinetics (Table 1). As already pointed out, Jennings and Solomon found a single binding affinity for the protein site, and a total number of protein sites that may exceed the number of sites at which charged phloretin competes for DBDS binding to band 3. Thus, it is not possible to rule out effects of uncharged phloretin on band 3, especially in view of the finding by Wieth et al. [19] that uncharged

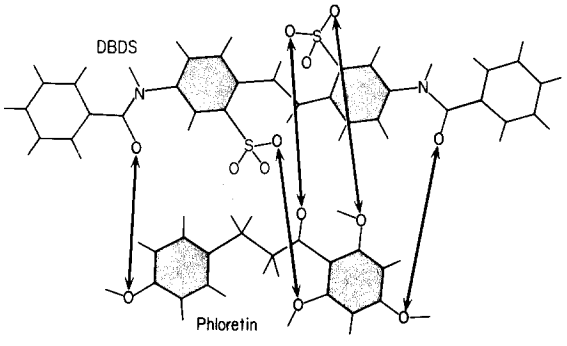

Fig. 8. Structural relationship between DBDS (top) and phloretin (bottom) drawn from Dreiding models. The double-headed arrows between the oxygens indicate regions of structural similarity. Analogous benzene rings have been stippled. Both molecules have a great deal of rotational freedom but can adopt essentially planar conformations except for the hydrogens at the phloretin double bond and the oxygens in the DBDS sulfate groups.

phloretin may be responsible for inhibition of anion exchange.

Acknowledgements

We should like to express our appreciation for the essential contributions of Dr. Alfred Pandiscio and Mr. Bernard Corrow to the design and construction of the experimental apparatus. One of us (A.S.V.) wishes to acknowledge a Medical Scientist Scholarship donated by the Prudential Insurance Co. This work was supported in part by grants NIH 2 R01 HL14820 and 5 R01 GM15692.

References

1 Owen, J.D. and Solomon, A.K. (1972) Biochim. Biophys. Acta 290, 414–418
2 Wieth, J.O., Dalmark, M., Gunn, R.B. and Tosteson, D.C. (1972) in Erythrocytes, Thrombocytes, Leucocytes (Gerlach, E., Moser, K., Deutsch, E. and Wilmanns, W., eds.), pp. 71–76, Georg Thieme Verlag, Stuttgart
3 Macey, R.E. and Farmer, R.E.L. (1970) Biochim. Biophys. Acta 211, 104–106
4 Lefevre, P.G. and Marshall, J.K. (1959) J. Biol. Chem. 234, 3022–3026.
5 Kupta, R.M. (1971) Biochemistry 10, 1143–1153
6 Jennings, M.L. and Solomon, A.K. (1976) J. Gen. Physiol. 67, 381–397
7 Knauf, P.A. (1979) Curr. Top. Membrane Trans. 12, 249–363
8 Rao, A., Martin, P., Reithmeier, R.A.F. and Cantley, L.C. (1979) Biochemistry 18, 4505–4516
9 Verkman, A.S., Dix, J.A. and Solomon, A.K. (1982) J. Gen. Physiol., in the press
10 Kotaki, M., Naoi, R. and Yagi, R. (1971) Biochim. Biophys. Acta 249, 547–566.
11 Dodge, J.T., Mitchell, C. and Hanahan, D.T. (1963) Arch. Biochem. Biophys. 100, 119–130
12 Schnell, K.F., Besl, E. and Manz, A. (1978) Pflüger's Arch. 375, 87–59
13 Lowry, O.H., Rosebrough, N.J., Farr, A.L. and Randall, R.J. (1951) J. Biol. Chem. 193, 265–275
14 Verkman, A.S., Pandiscio, A.A., Jennings, M. and Solomon, A.K. (1980) Anal. Biochem. 102, 189–195
15 Verkman, A.S. (1980) Ph.D. Thesis, Harvard University
16 Kleinfeld, A.M., Pandiscio, A.A. and Solomon, A.K. (1979) Anal. Biochem. 94, 65–74
17 Verkman, A.S., Dix, J.A. and Solomon, A.K. (1982) Biophys. J. 37, 216a
18 Verkman, A.S. and Dix, J.A. (1981) Biophys. J. 33, 188a
19 Wieth, J.O., Funder, J., Gunn, R.B. and Brahm, J. (1974) in Comparative Biochemistry and Physiology of Transport (Bolis, L., Bloch, K., Luria, S.E. and Lynen, F., eds.), pp. 317–337, North-Holland, Amsterdam
20 Cousin, J.L. and Motais, R. (1977) Biochim. Biophys. Acta 507, 531–538
21 Andersen, O.S., Finkelstein, A., Katz, I. and Cass, A. (1976) J. Gen. Physiol. 67, 749–771
22 Melnik, E., Latorre, R., Hall, J.E. and Tosteson, D.C. (1977) J. Gen. Physiol. 69, 243–257
23 Verkman, A.S. and Solomon, A.K. (1980) J. Gen. Physiol. 75, 673–692
24 Macara, I.G. and Cantley, L.C. (1981) Biochemistry 20, 5695–5701